Asian Journal of Chemistry; Vol. 33, No. 4 (2021), 937-944

ASIAN JOURNAL OF CHEMISTRY

https://doi.org/10.14233/ajchem.2021.23068

# Free Radical Scavenging Activity of Dihydrocaffeic Acid: A Quantum Chemical Approach

K. SENTHILKUMAR[1], S.S. NAINA MOHAMMED[1] and S. KALAISELVAN[2,*]

[1]Department of Physics, Government Arts College, Udumalpet, Tirupur-642126, India
[2]Department of Chemistry, M. Kumarasamy College of Engineering, Karur-639113, India

*Corresponding author: E-mail: kalaichem82@gmail.com

*Received*: 16 November 2020; *Accepted*: 25 February 2021; *Published online*: 20 March 2021; AJC-20307

Based on density functional theory (DFT), to investigate relationships between the antioxidant activity and structure of dihydrocaffeic acid, quantum chemical calculation is used. The optimized structures of the neutral, radical and ionic forms have been carried out by DFT-B3LYP method with the 6-311G(d,p) basis set. Reaction enthalpies related with the hydrogen atom transfer (HAT), single electron transfer proton transfer (SET-PT) and sequential proton loss and electron transfer (SPLET) were calculated in gas and water phase. The HOMO-LUMO energy gap, electron affinity, electronegativity, ionization energy, hardness, chemical potential, global softness and global electrophilicity were calculated by using the same level of theory. Surfaces with a molecular electrostatic potential (MEP) were studied to determine the reactive sites of dihydrocaffeic acid. The difference in energy between the donor and acceptor as well as the stabilization energy was determined through the natural bond orbital (NBO) analysis. The Fukui index (FI) based on electron density was employed to predict reaction sites. Reaction enthalpies are compared with previously published data for phenol and 3,4-dihydroxycinnamic acid.

**Keywords: Density functional theory, Dihydrocaffeic acid, Fukui index.**

## INTRODUCTION

Dihydrocaffeic acid or 3-(3,4-dihydroxyphenyl)propenoic acid is acquired from plants species, such as *Gynura bicolor* [1], *Nepeta teydea* [2] and *Selaginella stautoniana* [3]. Moreover, dihydrocaffeic acid is also present in the common beet, red beetroot and olives. Additionally, dihydrocaffeic acid is a caffeic acid metabolic product and researched due to its potent antioxidant properties has been detected in human plasma after coffee ingestion [4]. The chemical compounds called antioxidants can inhibit oxidative reactions and trap the intermediates of free radicals produced during an oxidative reaction. Natural antioxidants have received considerable attention because these antioxidants can significantly reduce or altogether prevent biomolecule oxidation through free radicals [5,6]. Biomolecule oxidation is closely related to the progression and initiation of various diseases including cardiovascular disease, atherosclerosis, cancer and neurodegenerative disease as well as ageing [7,8].

Computational methodologies and quantum chemistry provide the energy information and atomic-level structures of systems with the accuracy greater than or equivalent to the experimentally obtained accuracy. Therefore, for the investigation of underlying drug structure-activity relationships and rational design of novel potential drugs, theoretical calculations are widely employed as a cogent tool [9]. Several examples of design of new antioxidants [10-12] by employing economical and powerful quantum chemical methods, especially DFT and successful rational interpretation of the structure-activity relationships of naturally obtained antioxidants [9,13-16] are reported. Five thermodynamic parameter sets, namely ionization potential (IP), bond dissociation enthalpy (BDE), proton dissociation enthalpy, electron transfer enthalpy and proton affinity, were identified using the high-precision DFT calculation. These parameters were used to determine three working mechanisms of single electron transfer proton transfer, hydrogen atom transfer (HAT) and sequential proton loss and electron transfer (SPLET) under various microenvironments (water and gas phase). In free radicals, to understand the radical scavenging reactivity of investigated molecules, the spin density and lowest unoccupied molecular orbital (LUMO) and highest occupied molecular orbital (HOMO) distributions were calculated. Additionally, the molecular electrostatic potential (MEP) and Fukui index (FI) of dihydrocaffeic acid were determined. In

this study, structural insights into the mechanisms of action of phenolics were obtained. These insights may aid expand the applications of phenolics to food and pharmaceutical sciences.

## COMPUTATIONAL METHODS

**Theoretical background and computational details:** All electronic calculations were performed with the Gaussian 03 program package [17]. The geometry optimization of dihydrocaffeic acid molecule and respective radicals, radical cations and anions was performed using DFT method with B3LYP functional [18,19] and the 6-311G** basis set [18] in the gas phase and water. Single point energy calculations were performed by the same level of theory. The optimized structures were confirmed to be real minima by potential energy surface scans without imaginary frequencies. The conformer with the lowest energy was used in this work. All reported enthalpies were zero point corrected with non-scaled frequencies. Total enthalpies were calculated at 298.15 K and 1.0 atmospheric pressure. The natural bond orbital (NBO) analysis were performed on dihydrocaffeic acid by the NBO 3.1 program [20] at the B3LYP/6-311G(d,p) level as implemented in the Gaussian 03 program software package [17]. Solvent contribution to the total enthalpies was computed employing integral equation formalism (IEF-PCM) method [21,22]. Gaussian 03 can provide solution-phase geometry optimization; thus, the Gaussian 03 approach was employed for radicals (radical anion and cation) and the parent molecule. All the IEF-PCM calculations were conducted using default Gaussian program package setting. The IP is calculated as the energy difference between radical cation ($E_c$) and the respective neutral molecule ($E_n$). The EA is calculated as the difference between a radical anion ($E_a$) and the respective neutral molecule ($E_n$). These two terms IP and EA are useful to define the measurement of global reactivity descriptors [(electronegativity ($\chi$), global hardness ($\eta$), global softness (S) and electrophilicity index ($\omega$)] according to Geerlings *et al.* [23]. Based on the theoretical approach of DFT, Janak's theorem and the finite difference approximation, these descriptors can be proposed by $IP_o = -E_{HOMO}$ and $EA_o = -E_{LUMO}$ [24]. The electrodonating ($\omega-$) and electroaccepting ($\omega+$) power as formulated by Gazquez *et al.* [25].

## RESULTS AND DISCUSSION

**Conformational analysis and geometrical structures:** To elucidate the relationship between the molecular structure and antioxidant activity, the conformational and geometrical features are significant. Potential energy profile of dihydrocaffeic acid as a function of the torsion angle ($\tau$) around the $C_4$-$C_7$ bond have been characterized by exploring in steps of 5° ranging from -60° to 300° at B3LYP/6-311G(d,p) level of theory in gas phase. The plot of potential energy profile is presented in Fig. 1. The minimization procedure for dihydrocaffeic acid yields a non-planar conformation at $\tau = 75°$, is the more stable one. This absolute minimum is followed by relative minimum at $\tau = 255°$ with a potential barrier of 134.5 kcal/mol. The potential energy maximum lies at $\tau = -50°$ and 195°, respectively and the energy difference between maxima and minima

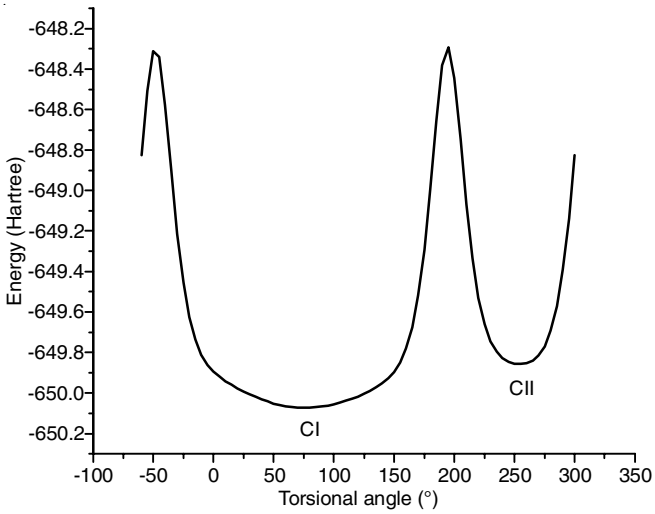


Fig. 1. Potential energy surface scan of dihydrocaffeic acid calculated at B3LYP/6-311G** protocol

is about 1104.66 kcal/mol. After the minimum energy conformations further geometry optimization was performed with the same level of theory. Geometries of neutral forms, anions, radicals and radical cations have been found in the energy minima at B3LYP/6-311G(d,p) level of theory. Harmonic vibrational frequencies were computed for all molecules (acid, ionic species and radicals) to characterize all their conformations as minimum energy points with the absence of imaginary frequencies and to evaluate the zero-point energy (ZPE) corrections, included in bond dissociation energies.

Fig. 2a-c displays the optimized structure of dihydrocaffeic acid and their radicals calculated in gas phase at the B3LYP/6-311G (d,p) level of theory and atom numberings of dihydrocaffeic acid is shown in Fig. 3. The optimized geometrical parameters for neutral molecule, 3–OH radical, 4–OH radical, cation radical and anion are collected in Table-1. By comparison, it can be seen that no significant geometrical change has been observed when going from the neutral molecule to the phenoxy (ArO) and cation ($ArOH^+$) radicals as well as anion forms ($ArOH^-$). While the largest deviation in torsion angle (C4-C7-C8-C9) by 16.92°, due to charge conjugation on the cationic species. An intramolecular hydrogen bond (IHB) between the 3-hydroxyl hydrogen and the 4-carbonyl oxygen was found with bond length of 1.9979 Å. The stabilization of the radical lowers the BDE and increases the antioxidant activity of the dihydrocaffeic acid. From the observed values of total electronic energies 4-OH radical is more stable than the 3-OH ($\Delta E = 9.94$ kcal/mol). The stability of free radical was enhanced due to the presence of electron withdrawing group (-COOH) in the propenoic moiety and electron donating group (-OH) present at the *ortho*-position resulted in the stability increase of the radical by resonance [26]. The bond order and bond length of various structural parameters of the studied compound is listed in Table-2. Smaller bond orders represents weaker bond. The values of bond order and bond length are opposite except for O-H group. Accordingly, phenolic hydroxyl in propenoic moiety may be active site because O10–H21 has the smallest bond order and largest bond

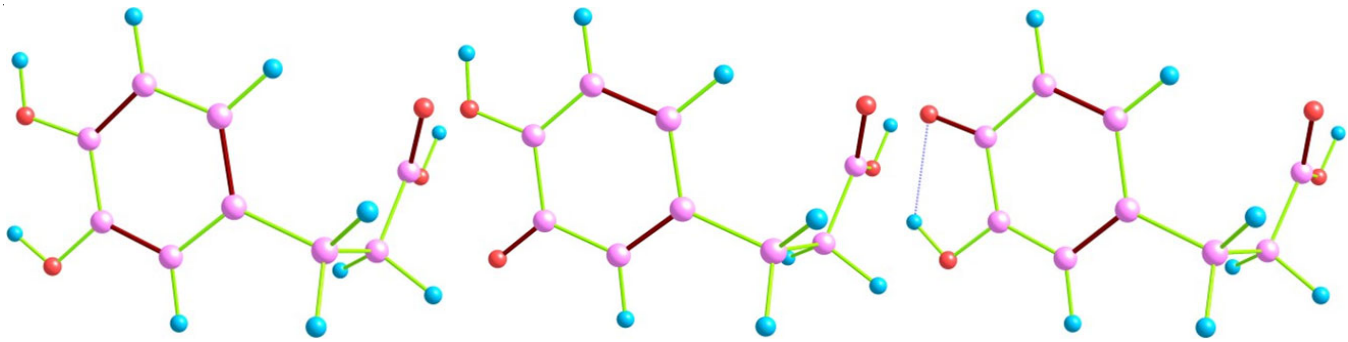

(a) Dihydrocaffeic acid – Neutral molecule (b) Dihydrocaffeic acid 3-OH Radical (c) Dihydrocaffeic acid 4-OH Radical

Fig. 2(a-c). Optimized structures of dihydrocaffeic acid and their radicals at B3LYP/6-311G** level of theory

TABLE-1
SELECTED GEOMETRICAL PARAMETERS OF DIHYDROCAFFEIC ACID, RADICAL AND IONIC SPECIES USING DFT/B3LYP/6-311G** METHOD

| S. No. | Structural parameter | Neutral | 3-OH Radical | 4-OH Radical | Anionic species | Cationic species |
|---|---|---|---|---|---|---|
| | | | Bond length (Å) | | | |
| 1 | C1-C2 | 1.401 | 1.374 | 1.398 | 1.429 | 1.382 |
| 2 | C2-C3 | 1.389 | 1.449 | 1.386 | 1.399 | 1.397 |
| 3 | C3-C4 | 1.403 | 1.470 | 1.467 | 1.389 | 1.451 |
| 4 | C4-C5 | 1.387 | 1.388 | 1.438 | 1.421 | 1.392 |
| 5 | C5-C6 | 1.396 | 1.393 | 1.370 | 1.404 | 1.380 |
| 6 | C6-C1 | 1.396 | 1.422 | 1.427 | 1.393 | 1.442 |
| 7 | C4-C7 | 1.515 | 1.516 | 1.511 | 1.510 | 1.506 |
| 8 | C7-C8 | 1.538 | 1.538 | 1.540 | 1.533 | 1.542 |
| 9 | C8-C9 | 1.513 | 1.512 | 1.513 | 1.502 | 1.513 |
| 10 | C9-O10 | 1.354 | 1.352 | 1.352 | 1.383 | 1.334 |
| 11 | C3-O12 | 1.363 | 1.244 | 1.332 | 1.381 | 1.318 |
| 12 | C4-O13 | 1.379 | 1.344 | 1.253 | 1.408 | 1.331 |
| 13 | C9-O11 | 1.205 | 1.206 | 1.205 | 1.223 | 1.212 |
| 14 | C2-H14 | 1.085 | 1.085 | 1.084 | 1.085 | 1.083 |
| 15 | C5-H15 | 1.086 | 1.087 | 1.083 | 1.085 | 1.084 |
| 16 | C3-H16 | 1.083 | 1.083 | 1.083 | 1.087 | 1.081 |
| 17 | C7-H17 | 1.092 | 1.093 | 1.092 | 1.094 | 1.091 |
| 18 | C7-H18 | 1.094 | 1.093 | 1.093 | 1.104 | 1.094 |
| 19 | C8-H19 | 1.097 | 1.096 | 1.096 | 1.117 | 1.092 |
| 20 | C8-H20 | 1.092 | 1.093 | 1.093 | 1.092 | 1.095 |
| 21 | O10-H21 | 0.969 | 0.969 | 0.969 | 0.968 | 0.971 |
| 22 | O12-H22 | 0.966 | Nil | 0.981 | 0.970 | 0.972 |
| 23 | O13-H23 | 0.962 | 0.965 | Nil | 0.983 | 0.968 |
| | | | Bond angle (°) | | | |
| 24 | C1-C7-C8 | 113.8 | 114.1 | 113.8 | 113.0 | 113.6 |
| 25 | C6-C1-C7 | 121.3 | 120.5 | 120.3 | 121.9 | 119.8 |
| | | | Dihedral angle (°) | | | |
| 26 | C1-C7-C8-C9 | 75.38 | 76.02 | 76.87 | 78.16 | 58.46 |
| 27 | C6-C1-C7-C8 | -91.36 | -87.42 | -88.78 | -103.0 | -104.4 |

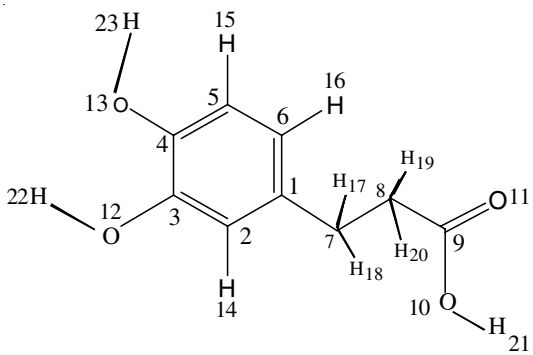


Fig. 3. Atom numbering of dihydrocaffeic acid

length. This is not consistent with theoretical values of bond dissociation enthalpy of hydroxyl groups in phenolic ring. Although O13–H23 bond order is larger than is O12–H22 and more active than the later. Hence, the bond order and bond length cannot be used to measure its bond strength and identify the location of active site on the molecule. So these two parameters are used to find the active site in the molecule to certain extent.

**Electronic properties:** To estimate the separation of positive and negative electrical charges, the dipole moment of dihydrocaffeic acid was found to be 1.8442 Debye. The dipole moment values of 4.32D and 3.83D for its 3-OH and 4-OH radicals, respectively. The high dipole moments accompanied

TABLE-2
BOND ORDER AND BOND LENGTH VALUES OF DIHYDROCAFFEIC ACID CALCULATED AT B3LYP/6-311G** LEVEL OF THEORY

| S. No. | Structural parameters | BD | BD* | Bond order | Bond length |
|---|---|---|---|---|---|
| 1 | C1-C2 | 1.9699 | 0.0229 | 0.9735 | 1.401 |
| 2 | C2-C3 | 1.9722 | 0.0220 | 0.9751 | 1.389 |
| 3 | C3-C4 | 1.9723 | 0.0403 | 0.9660 | 1.403 |
| 4 | C4-C5 | 1.9768 | 0.0257 | 0.9755 | 1.387 |
| 5 | C5-C6 | 1.9719 | 0.0153 | 0.9783 | 1.396 |
| 6 | C6-C1 | 1.9719 | 0.0246 | 0.9737 | 1.396 |
| 7 | C4-C7 | 1.9721 | 0.0231 | 0.9745 | 1.515 |
| 8 | C7-C8 | 1.9707 | 0.0164 | 0.9772 | 1.538 |
| 9 | C8-C9 | 1.9803 | 0.0641 | 0.9580 | 1.513 |
| 10 | C9-O10 | 1.9952 | 0.0996 | 0.9478 | 1.354 |
| 11 | C3-O12 | 1.9926 | 0.0202 | 0.9862 | 1.363 |
| 12 | C4-O13 | 1.9923 | 0.0242 | 0.9841 | 1.379 |
| 13 | C9-O11 | 1.9966 | 0.0231 | 0.9867 | 1.206 |
| 14 | C2-H14 | 1.9763 | 0.0137 | 0.9813 | 1.085 |
| 15 | C5-H15 | 1.9766 | 0.0141 | 0.9812 | 1.086 |
| 16 | C3-H16 | 1.9776 | 0.0145 | 0.9816 | 1.083 |
| 17 | C7-H17 | 1.9774 | 0.0138 | 0.9818 | 1.092 |
| 18 | C7-H18 | 1.9755 | 0.0123 | 0.9816 | 1.094 |
| 19 | C8-H19 | 1.9570 | 0.0119 | 0.9726 | 1.097 |
| 20 | C8-H20 | 1.9733 | 0.0130 | 0.9802 | 1.092 |
| 21 | O10-H21 | 1.9869 | 0.0111 | 0.9879 | 0.969 |
| 22 | O12-H22 | 1.9879 | 0.0107 | 0.9886 | 0.966 |
| 23 | O13-H23 | 1.9890 | 0.0073 | 0.9909 | 0.962 |

with the high charge densities and high polarity in bonds [27]. The average polarizability of dihydrocaffeic acid was computed as 329.4 a.u. indicating their solubility in polar solvents and ability of polarizing other atoms or molecules. The isotropic polarizabilities and polarizabilities anisotropy invariants were also calculated for dihydrocaffeic acid at the same level of theory. The calculated anisotropy of the polarizability and first order hyperpolarizability is 108.2 and 499.4 a.u., respectively, thus indicating that this compound is a good candidate of non-linear optical material (Table-3). The global descriptors such as, chemical hardness (η) is the reluctance towards the deformation, softness (S) is inversely proportional to hardness, chemical potential (μ) is the escaping tendency of electron from equilibrium and negative of electronegativity (χ) and electrophilic index (ω) is strength of electrophilicity of the species. The global reactive descriptors of dihydrocaffeic acid are presented in Table-4. The calculated value of ionization potential, hardness and electronegativity by energy-vertical method is higher than the values obtained by orbital-vertical. Molecular descriptor results show that the system does not lose electrons easily and a low electron affinity tends to donate electrons easily due to a high ionization potential. The more resistance to charge transfer is observed in dihydrocaffeic acid due to non-planar configuration is revealed from the measured hardness values by both the methods. The value of softness and electron donating power obtained by $E_V$ and $O_v$ method agreed very well with a difference of 0.06 and 0.01 eV, respectively. The calculated electronic descriptors clearly confirmed that dihydrocaffeic acid acts as electron donor rather than electron acceptor and it is an indication of antioxidant capability.

TABLE-3
ELECTRIC DIPOLE-MOMENT, POLARIZABILITY AND HYPERPOLARIZABILITY OF THE TITLE COMPOUND AT B3LYP/6-311G** LEVEL OF THEORY

| Parameter | Value (a.u) | Parameter | Value (a.u) |
|---|---|---|---|
| $\mu_x$ | 0.2549 | $\beta_{xxx}$ | -326.5603044 |
| $\mu_y$ | 1.6081 | $\beta_{xxy}$ | -12.2661303 |
| $\mu_z$ | 0.866 | $\beta_{xyy}$ | -97.1967618 |
| $\mu_{total}$ | 1.8442 | $\beta_{yyy}$ | 3.5081446 |
| $\alpha_{xx}$ | 134.7988817 | $\beta_{xxz}$ | -38.3984892 |
| $\alpha_{xy}$ | 5.0970045 | $\beta_{xyz}$ | -23.0015466 |
| $\alpha_{yy}$ | 114.6467899 | $\beta_{yyz}$ | -26.0314791 |
| $\alpha_{xz}$ | 12.7739292 | $\beta_{xzz}$ | -65.071289 3 |
| $\alpha_{yz}$ | -3.6864643 | $\beta_{yzz}$ | 9.675433 |
| $\alpha_{zz}$ | 75.168816 | $\beta_{zzz}$ | -37.805849 |
| $\alpha_0$ | 108.2048292 | $\beta_0$ | 499.405812 |

TABLE-4
ELECTRONIC PROPERTIES OF DIHYDROCAFFEIC ACID CALCULATED AT B3LYP/6-311G** LEVEL OF THEORY

| Electronic descriptors | Electronic energy (eV) | Orbital energy (eV) |
|---|---|---|
| IP | 7.4653 | 5.7816 |
| EA | -0.9205 | 0.1774 |
| H | 4.1929 | 2.8021 |
| X | 3.2724 | 2.9795 |
| S | 0.1192 | 0.1784 |
| Ω | 1.2770 | 1.5841 |
| $\omega^-$ | 3.4373 | 3.4241 |
| $\omega^+$ | 0.1649 | 0.4446 |
| $\Delta\omega^{\pm}$ | 3.6022 | 3.8687 |

**Analysis of reaction enthalpies:** Calculated gas and water phase B3LYP/6-311G** reaction enthalpies are summarized in Table-5. The calculated gas phase BDE value of 4-OH radical is lower than 3-OH radical by 40KJ/mol. The calculated gas phase BDE of 4-OH radical is 301.85KJ/mol that was lower than the experimental results of tocopherols [28-30] and computational results of phenol [31]. Position 4 is the preferred site for radical inactivation because of its lowest energy requirements lowest BDE, (IP+PDE) and (PA+ETE) in gas and water phases. The 4-OH BDE value is lower by 5.84 KJ/mol [32] in 3,4-dihydroxycinnamic acid with B3LYP/6-31+G** level of theory. The calculated gas phase ionization potential and proton affinities are significantly higher than their O-H BDEs, therefore HAT represents the thermodynamically preferred pathway. The obtained gas phase IP is lower than IP of phenol [31]. This indicates that the electron donating substitution on phenyl ring lowers the IP. The lowering of IP reveals the stronger electron donating ability than that of phenol. The calculated water phase reaction enthalpies revealed that PAs are lower than 92% and 96% of the BDEs of 3-OH and 4-OH radical, respectively. Therefore SPLET mechanism represents the thermodynamically favoured process in water. The calculated value of ionization potential in water phase is dramatically lower than in the gas phase. This confirms that the solvent can facilitate electron donation. From the published results, dihydrocaffeic acid had higher capacity than quercetin [33] and α-tocopherol [34] in $DPPH^{\bullet}$ assay. Hence, the obtained theoretical reaction enthalpies

TABLE-5
REACTION ENTHALPIES OF DIHYDROCAFFEIC ACID IN GAS AND WATER PHASE CALCULATED AT B3LYP/6-311G** LEVEL OF THEORY (VALUES ARE IN KJ/mol)

| Species | Gas phase | | | | | Water phase | | | | |
|---|---|---|---|---|---|---|---|---|---|---|
| | BDE | PDE | PA | ETE | IP | BDE | PDE | PA | ETE | IP |
| 3-OH radical | 341.85 | 941.03 | 1478.05 | 172.97 | – | 331.19 | 25.63 | 177.82 | 270.69 | – |
| 4-OH radical | 301.85 | 901.03 | 1417.51 | 193.51 | – | 318.31 | 12.74 | 153.89 | 281.74 | – |
| Dihydrocaffeic acid | – | – | – | – | 716.12 | – | – | – | – | 422.88 |

elucidate that the target molecule has a potential antioxidant capacity.

**Molecular electrostatic potential:** For the nucleophilic and electrophilic attacks, charge distributions over the appropriate regions and molecules were visualised through MEP map [35]. Various electrostatic potential values are denoted using different colours. High electron density areas are indicated with red surfaces and low electron density regions are represented using blue surfaces. The following is the increasing electron density order: red < orange < yellow < green < blue. The MEP plots of dihydrocaffeic acid (Fig. 4) indicate the existence of oxygen atoms on the hydroxyl group of maps (characterized using the red colour). These plots are considered the most negative potential regions. In hydroxyl groups, the existence of hydrogen atoms is represented with the blue region having the positive charge.

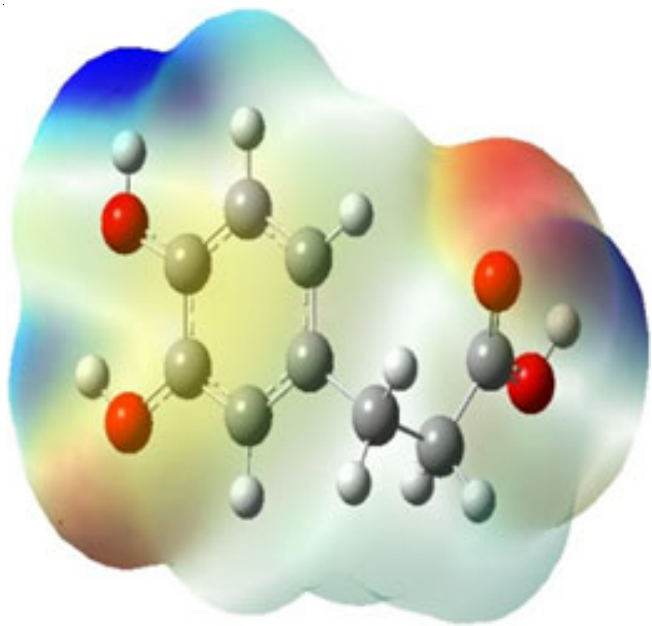

Fig. 4. MEP plot of dihydrocaffeic acid using B3LYP/6-311G**

In dihydrocaffeic acid, the MEP surface colour code varied between the deep red (-0.04291 a.u.) and deep blue (0.04291 a.u.). For the electrophilic attack on oxygen atoms, the most probable sites are 4-OH, 3-OH and C=O groups. The high-electrophilic reactivity obtained from weak electron density on the hydrogen atom and electron concentrations on the oxygen atom indicates the nucleophilic attack. The MEP analysis also projects superior charge localization on hydroxyl group at 3-OH site and acts as a preferred interaction site for free radical scavenging activity.

**Frontier molecular orbital and Fukui index analysis:** Frontier orbital distribution and energy are crucial parameters for understanding the free radical scavenging activity of phenolic antioxidants. In an electronic transition, HOMO and LUMO are the primary participants, and the energy gap between HOMO and LUMO depicts reactivity [36]. Conjugated molecules are analyzed through the small HOMO-LUMO separation. This separation results from a large transfer of intramolecular charges from the end-capping electron-donor to electron-acceptor groups. This transfer occurs through a π-conjugated path [37]. The energy gap ($E_g$) between HOMO and LUMO obtained from the correlation functional B3LYP is found to be 5.6 eV and hence lesser the energy gap the higher will be the structural activity. The HOMO and LUMO of dihydrocaffeic acid were explored at the B3LYP/6-311G(d,p) level of DFT and plots are shown in Fig. 5(a-f). In dihydrocaffeic acid and 4-OH$^{\bullet}$, HOMO of π-nature is delocalized over the benzene ring, as well as C7-C8 bond. For 3-OH radical the HOMO is delocalized over the benzene ring only. Whereas in LUMO, the charge delocalization are over the entire molecule for all the three species. Comparing the LUMO of two radicals, 4–O$^{\bullet}$ site is delocalized more with respect to 3–O$^{\bullet}$ site. The HOMO distribution of the phenolic oxygen atom is larger than others (Fig. 5). Hence, the OH groups on the phenyl ring would be more easily attracted by free radicals.

In addition to the considerations of frontier molecular orbitals, Fukui indices are one of the most crucial parameters. Fukui indices can be a spontaneous solution for justifying the powerful reactive sites of all the atoms. Okada *et al*. [24] reported that the maximum $f_k^+$ and $f_k^-$ of positive and negative charges, respectively, correspond to electrophilic and nucleophilic attractive sites. Table-6 presents the Fukui indices calculated in a gaseous medium on the basis of the theoretical HSAB principle [38]. From the obtained results, C7 is the best site for nucleophilic attack and O12 is the best site for the electrophilic attack. The Fukui site prediction in the dihydrocaffeic acid reveals that the electrophilic site is concentrated over phenyl ring and nucleophilic site is concentrated over propenoic moiety. A large positive value of condensed Fukui descriptor is over C7 followed by C6, C3, C1 and C4 atoms are preferred as nucleophilic sites and hence act as electron donating areas for radical scavenging activity.

**Spin density analysis:** Antioxidants are important because of their ability to terminate chain reactions that can lead to diseases. In free-radical scavenging, antioxidants become free radicals; however, they do not initiate a chain reaction because of their stability. The stability of the free radical produced plays a key role in a compound's antioxidant activity. Thus, the spin

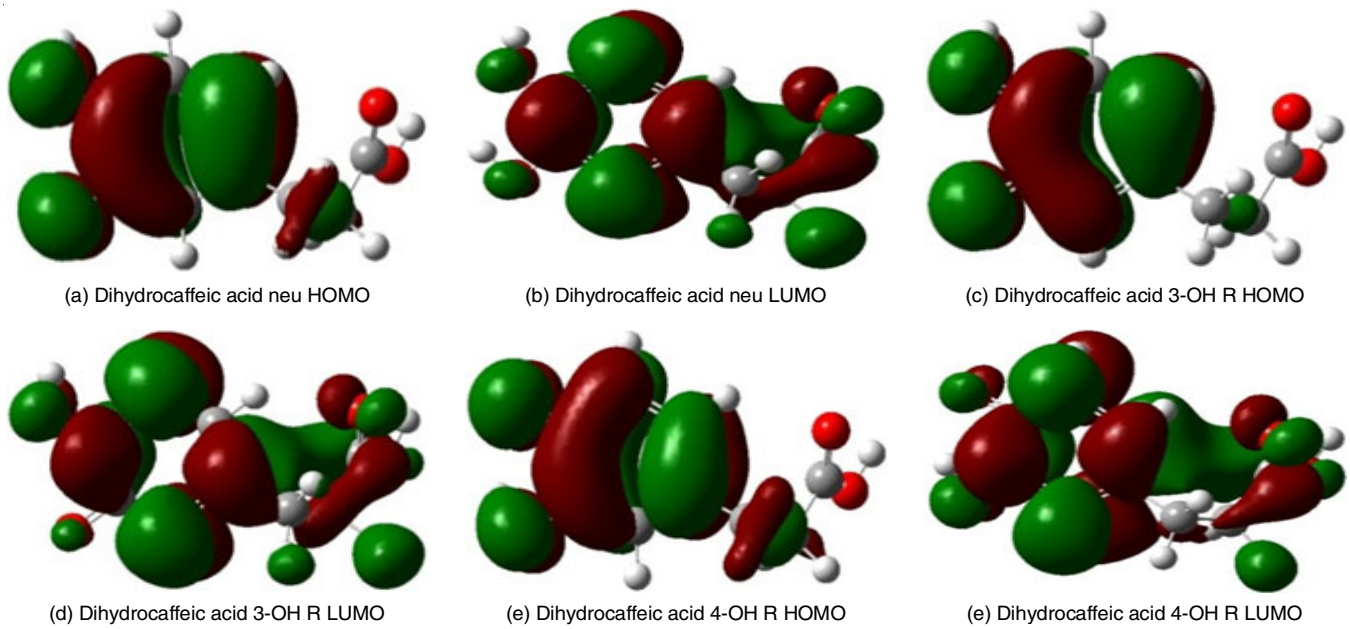

(a) Dihydrocaffeic acid neu HOMO (b) Dihydrocaffeic acid neu LUMO (c) Dihydrocaffeic acid 3-OH R HOMO

(d) Dihydrocaffeic acid 3-OH R LUMO (e) Dihydrocaffeic acid 4-OH R HOMO (e) Dihydrocaffeic acid 4-OH R LUMO

Fig. 5(a-f). HOMO-LUMO plots of dihydrocaffeic acid and their radicals calculated at B3LYP/6-311G** level of theory

TABLE-6
CONDENSED FUKUI FUNCTION CALCULATIONS OF DIHYDROCAFFEIC ACID AT B3LYP/311G** LEVEL OF THEORY

| Atom | $f_k^+$ | $f_k^-$ | $f_k^0$ | $\Delta f$ |
|---|---|---|---|---|
| C1 | 0.001 | -0.021 | -0.010 | 0.022 |
| C2 | -0.078 | -0.044 | -0.061 | -0.034 |
| C3 | 0.010 | -0.048 | -0.019 | 0.058 |
| C4 | -0.038 | -0.058 | -0.048 | 0.02 |
| C5 | -0.104 | -0.041 | -0.073 | -0.063 |
| C6 | -0.001 | -0.110 | -0.056 | 0.109 |
| C7 | 0.398 | -0.010 | 0.194 | 0.408 |
| C8 | 0.049 | 0.025 | 0.037 | 0.024 |
| C9 | -0.042 | -0.023 | -0.033 | -0.019 |
| O10 | -0.040 | -0.034 | -0.037 | -0.006 |
| O11 | -0.070 | -0.001 | -0.036 | -0.069 |
| O12 | -0.043 | -0.118 | -0.081 | 0.075 |
| O13 | -0.033 | -0.090 | -0.062 | 0.057 |
| H14 | -0.053 | -0.059 | -0.056 | 0.006 |
| H15 | -0.045 | -0.062 | -0.054 | 0.017 |
| H16 | -0.054 | -0.047 | -0.051 | -0.007 |
| H17 | -0.033 | -0.021 | -0.027 | -0.012 |
| H18 | -0.071 | -0.050 | -0.061 | -0.021 |
| H19 | -0.116 | -0.041 | -0.079 | -0.075 |
| H20 | -0.023 | -0.024 | -0.024 | 0.001 |
| H21 | -0.045 | -0.029 | -0.037 | -0.016 |
| H22 | -0.045 | -0.042 | -0.044 | -0.003 |
| H23 | -0.137 | -0.051 | -0.094 | -0.086 |

densities of free radicals generated through antioxidants after hydrogen atom abstraction must be calculated. Furthermore, spin densities can provide the speed-related information of free-radical scavenging. The more delocalization in the spin density results in the easier radical formation and results in the faster scavenging reactions. Spin density is directly accosted to BDE because a low spin density leads to a decrease in BDE [39]. Moreover, spin densities can provide information of the reactivity of different active sites of a molecule. The spin densities of the O atoms of dihydrocaffeic acid, 4-OH and 3-OH were 0.364 and 0.380, respectively. The more delocalized is the spin density, the lower is the BDE and the more stabilized is the free radical. The 4-OH group, where the hydrogen atom abstracts, exhibits low spin density because of strong intramolecular hydrogen bonding and aromatic rings. These factors lead to an increase in the radical stability and a decrease in electron density from oxygen atom. Antioxidant activity of dihydrocaffeic acid is due to 4-OH group with lower BDE and spin density values. Obtained results show that in the gaseous phase, the lower spin density values will be proportional with the lower BDE values and superiority of spin density distribution over Fukui indices in determining the preferred point of interaction and as descriptors of phenolic antioxidant activity.

**NBO analysis:** An efficient approach for studying intra- and inter-molecular hydrogen bonding and an extended convenient foundation for studying conjugative interactions or charge transfer in molecular systems [40] through second-order perturbation theory were acquired through the NBO analysis. The second-order Fock matrix was studied to evaluate changes in the electron density of antibonding orbitals and interactions between acceptor and donor occupancies. Moreover, E(2) energy was investigated using the NBO analysis [41]. The results of the NBO analysis indicated the transfer of intermolecular charge from the bonding to antibonding orbitals. The most crucial interactions of empty (acceptor) non-Lewis NBOs with filled (donor) Lewis NBOs and the second-order perturbation energy (the stabilisation or interaction energy) of the most interactive NBOs of dihydrocaffeic acid are presented in Table-7. For each donor (i) and acceptor (j), the stabilization energy E(2) associated with the delocalization i, j is estimated as:

$$E^{(2)} = \Delta E_{ij} = q_i \frac{F(i,j)^2}{\varepsilon_j - \varepsilon_i}$$

TABLE-7
SECOND ORDER PERTURBATION INTERACTION ENERGY VALUES COMPUTED IN THE NBO BASIS FOR DIHYDRO-CAFFEIC ACID CALCULATED AT B3LYP/6-311G (d,p)

| Donor Lewis NBO (i) | Acceptor non- Lewis NBO (j) | E2 (KJ/mol) | $E_i$–$E_i$ (a.u.) | F(i,j) (a.u.) |
|---|---|---|---|---|
| $\sigma(C_6–C_1)$ | $\sigma^*(C_1–C_2)$ | 16.07 | 1.27 | 0.062 |
| $\sigma(C_6–C_1)$ | $\sigma^*(C_1–C_7)$ | 9.96 | 1.11 | 0.046 |
| $\sigma(C_6–C_1)$ | $\sigma^*(C_5–C_6)$ | 14.56 | 1.26 | 0.059 |
| $\sigma(C_6–C_1)$ | $\sigma^*(C_2–C_{14})$ | 10.92 | 1.13 | 0.049 |
| $\pi(C_6–C_1)$ | $\pi^*(C_2–C_3)$ | 79.96 | 0.27 | 0.066 |
| $\pi(C_6–C_1)$ | $\pi^*(C_4–C_5)$ | 86.44 | 0.27 | 0.068 |
| $\pi(C_4–C_5)$ | $\pi^*(C_6–C_1)$ | 74.18 | 0.31 | 0.068 |
| $\sigma(C_8–C_{19})$ | $\pi^*(C_9–C_{11})$ | 27.78 | 0.52 | 0.055 |
| $\pi(C_4–C_5)$ | $\pi^*(C_2–C_3)$ | 78.78 | 0.30 | 0.068 |
| $LP(2)O_{11}$ | $\sigma^*(C_8–C_9)$ | 77.82 | 0.65 | 0.100 |
| $LP(2)O_{11}$ | $\sigma^*(C_9–C_{10})$ | 135.98 | 0.62 | 0.128 |
| $LP(2)O_{10}$ | $\pi^*(C_9–C_{11})$ | 184.39 | 0.35 | 0.112 |
| $LP(2)O_{12}$ | $\pi^*(C_2–C_3)$ | 117.24 | 0.35 | 0.094 |
| $LP(2)O_{13}$ | $\pi^*(C_4–C_5)$ | 101.42 | 0.36 | 0.091 |

where $\varepsilon_i$ and $\varepsilon_j$ are the diagonal elements, $q_i$ is the donor orbital occupancy and F(i,j) is the off-diagonal NBO Fock matrix element. A larger E(2) value exhibits more intensive interactions of electron acceptors with electron donors. The tendency of donating electrons from donors to acceptors is relatively, more and the extent of entire system's conjugation is greater. Hyperconjugative interaction energies were determined using second-order perturbation. Electron density delocalization between unoccupied (Rydberg or antibonding) non-Lewis NBO orbitals and occupied Lewis (lone pair or bonding) NBO orbitals was attributed to stabilize the donor-acceptor interactions.

The $\pi^*\rightarrow\pi^*$ transitions have the higher resonance energies compared with other interactions of dihydrocaffeic acid such as C6-C1→C2-C3, C6-C1→C4-C5 and C4-C5→ C2-C3 with resonance energies E(2) of 79.96, 86.44 and 78.78 KJ/mol respectively, that lead to stability of dihydrocaffeic acid. The resonance energies of $\pi\rightarrow\pi^*$ transitions are higher than $\sigma\rightarrow\sigma^*$ transitions (Table-7). According to the $n\rightarrow\sigma^*$ and $n\rightarrow\pi^*$ interactions, the strongest interactions are due to n2(O11)→σ* (C9-O10), n2(O12)→π*(C2-C3) and n2(O10)→π*(C9-O11) with stabilization energies of 135.98, 117.24 and 184.39 KJ/mol, respectively. These findings revealed that a lone pair of electrons of oxygen atoms, particularly for phenolic hydroxyl groups, plays a key role in changing charge distribution structures, thereby significantly influencing the radical reactivity [42].

## Conclusion

Dihydrocaffeic acid have been investigated theoretically by DFT/B3LYP method with 6-311G(d, p) basis set to predict its molecular structure, electronic properties and radical scavenging activity. The hydrogen atom transfer (HAT) mechanism is easier for molecules with *ortho*-dihydroxy structure in phenyl ring. The presence of intramolecular hydrogen bonding (IHB) in 4-C=O point with adjacent hydrogen atom results in a 40 KJ/mol decrease in O-H BDE. In the gas phase, PAs and IPs are higher than BDEs. HAT denotes the thermodynamic preferred route. The results indicated that in water, the SPLET mechanism shows a thermodynamically favoured method. Molecular descriptor results showed that dihydrocaffeic acid is better electron donor rather than acceptor and is reported with negative electron affinity. The difference in the spin densities of the O atoms of 4-OH and 3-OH radicals was 0.016. On the benzene ring of 4-OH radical, the unpaired electron was delocalized. For radical inactivation, this site was preferred. The MEP map revealed that negative and positive potential sites were on electronegative atoms and around hydrogen atoms, respectively. This map provides the relative reactivity of atoms and the visual representation of chemically active sites. The FMO analyses indicated that charge transfer occurred within molecules. The energy gap between HOMO and LUMO showed molecule's chemical activity. The NBO analysis was conducted to evaluate the stability of molecules generated from the hyperconjugative interaction. The results showed that the intramolecular conjugative interaction led to the delocalization of π-electrons within the molecule. Non-bonding interactions occurred in the lone pair of electrons from the oxygen atom O10 to antibonding with 184.39 KJ/mol, increases the stability of a molecule. This theoretical study will be helpful for the development of more effective antioxidant and further exploitation for food and pharmaceutical applications.

## ACKNOWLEDGEMENTS

The authors thank Prof. Dr. R. Kumaresan for enlightening discussions and for computational facilities. The authors also acknowledge the Department of Physics, Government Arts College, Udumalpet, Tirupur, Tamilnadu, India for their constant encouragement and support.

## CONFLICT OF INTEREST

The authors declare that there is no conflict of interests regarding the publication of this article.

## REFERENCES

1. X. Zhou, M. Zhou, Y. Liu, Q. Ye, J. Gu and G. Luo, *Int. J. Food Prop.*, **19**, 233 (2016); https://doi.org/10.1080/10942912.2014.983607
2. B.M. Fraga, A. González-Coloma, S. Alegre-Gómez, M. López-Rodríguez, L.J. Amador and C.E. Díaz, *Phytochemistry*, **133**, 59 (2017); https://doi.org/10.1016/j.phytochem.2016.10.008
3. W.S. Feng, B. Zhu, X.K. Zheng, Y.L. Zhang, L.G. Yang and Y.J. Li, *Chin. J. Nat. Med.*, **9**, 108 (2011).
4. D.S. Goldstein, R. Stull, S.P. Markey, E.S. Marks and H.R. Keiser, *J. Chromatogr. B*, **311**, 148 (1984); https://doi.org/10.1016/S0378-4347(00)84701-5
5. W.A. Pryor, *Free Radic. Biol. Med.*, **28**, 141 (2000); https://doi.org/10.1016/S0891-5849(99)00224-5
6. M. Hahn, M. Baierle, M.F. Charão, G.B. Bubols, F.S. Gravina, P. Zielinsky, M.D. Arbo and S. Cristina Garcia, *Drug Chem. Toxicol.*, **40**, 368 (2017); https://doi.org/10.1080/01480545.2016.1212365
7. M. Dizdaroglu, P. Jaruga, M. Birincioglu and H. Rodriguez, *Free Radic. Biol. Med.*, **32**, 1102 (2002); https://doi.org/10.1016/S0891-5849(02)00826-2
8. A.C. Maritim, R.A. Sanders and J.B. Watkins, *J. Biochem. Mol. Toxicol.*, **17**, 24 (2003); https://doi.org/10.1002/jbt.10058

9. A.J. Javan, M.J. Javan and Z.A. Tehrani, *J. Agric. Food Chem.*, **61**, 1534 (2013); https://doi.org/10.1021/jf304926m
10. Y. Xue, Y. Zheng, L. An, Y. Dou and Y. Liu, *Food Chem.*, **151**, 198 (2014); https://doi.org/10.1016/j.foodchem.2013.11.064
11. G. Mazzone, N. Malaj, N. Russo and M. Toscano, *Food Chem.*, **141**, 2017 (2013); https://doi.org/10.1016/j.foodchem.2013.05.071
12. N. Nenadis, H.Y. Zhang and M.Z. Tsimidou, *J. Agric. Food Chem.*, **51**, 1874 (2003); https://doi.org/10.1021/jf0261452
13. J. Lengyel, J. Rimarcik, A. Vaganek and E. Klein, *Phys. Chem. Chem. Phys.*, **15**, 10895 (2013); https://doi.org/10.1039/c3cp00095h
14. J.S. Wright, E.R. Johnson and G.A. DiLabio, *J. Am. Chem. Soc.*, **123**, 1173 (2001); https://doi.org/10.1021/ja002455u
15. D.A. Pratt, G.A. DiLabio, G. Brigati, G.F. Pedulli and L. Valgimigli, *J. Am. Chem. Soc.*, **123**, 4625 (2001); https://doi.org/10.1021/ja005679l
16. M. Wijtmans, D.A. Pratt, L. Valgimigli, G.A. DiLabio, G.F. Pedulli and N.A. Porter, *Angew. Chem. Int. Ed.*, **42**, 4370 (2003); https://doi.org/10.1002/anie.200351881
17. M.J. Frisch, G.W. Trucks, H.B. Schlegel, G.E. Scuseria, M.A. Robb, J.R. Cheeseman, G. Scalmani, V. Barone, B. Mennucci, G.A. Petersson, H. Nakatsuji, M. Caricato, X. Li, H.P. Hratchian, A.F. Izmaylov, J. Bloino, G. Zheng, J.L. Sonnenberg, M. Hada, M. Ehara, K. Toyota, R. Fukuda, J. Hasegawa, M. Ishida, T. Nakajima, Y. Honda, O. Kitao, H. Nakai, T. Vreven, J.A. Montgomery Jr., J.E. Peralta, F. Ogliaro, J.J. Heyd, M. Bearpark, J.E. Brothers, K.N. Kudin, V.N. Staroverov, R. Kobayashi, J. Normand, K. Raghavachari, A. Rendell, J.C. Burant, S.S. Iyengar, J. Tomasi, M. Cossi, N. Rega, J.M. Millam, M. Klene, J.E. Knox, J.B. Ross, V. Bakken, C. Adamo, J. Jaramillo, R. Gomperts, R.E. Stratmann, O. Yazyev, A.J. Austin, R. Cammi, C. Pomelli, J.W. Ochterski, R.L. Martin, K. Morokuma, V.G. Zakrzewski, G.A. Voth, P. Salvador, J.J. Dannenberg, S. Dapprich, A.D. Daniels, O. Farkas, J.B. Foresman, J.V. Ortiz, J. Cioslowski and D.J. Fox, Gaussian 09, Revision D.01; Gaussian Wallingford, CT (2009).
18. A. Becke, *J. Chem. Phys.*, **98**, 5648 (1993); https://doi.org/10.1063/1.464913
19. C. Lee, W. Yang and R.G. Parr, *Phys. Rev. B Condens. Matter*, **37**, 785 (1988); https://doi.org/10.1103/PhysRevB.37.785
20. E.D. Glendening, J.K. Badenhoop, A.E. Reed, J.E. Carpenter, J.A. Bohmann and C.M. Morales, Weinhold F. *NBO 3.1* Theoretical Chemistry Institute and Department of Chemistry, University of Wisconsin, Madison, USA (2001).
21. J. Tomasi and M. Persico, *Chem. Rev.*, **94**, 2027 (1994); https://doi.org/10.1021/cr00031a013
22. V. Barone, M. Cossi and J.A. Tomasi, *J. Chem. Phys.*, **107**, 3210 (1997); https://doi.org/10.1063/1.474671
23. P. Geerlings, F. De Proft and W. Langenaeker, *Chem. Rev.*, **103**, 1793 (2003); https://doi.org/10.1021/cr990029p
24. T. Okada, M. Yamakawa, N. Ohmori, S. Mori, H. Horikawa, T. Hayashi and S. Fujishima, *Chem. Cent. J.*, **4**, 1 (2010); https://doi.org/10.1186/1752-153X-4-1
25. J.L. Gazquez, A. Cedillo and A. Vela, *J. Phys. Chem. A*, **111**, 1966 (2007); https://doi.org/10.1021/jp065459f
26. M. Leopoldini, T. Marino, N. Russo and M. Toscano, *J. Phys. Chem. A*, **108**, 4916 (2004); https://doi.org/10.1021/jp037247d
27. K. Sadasivam and R. Kumaresan, *Spectrochim. Acta A Mol. Biomol. Spectrosc.*, **79**, 282 (2011); https://doi.org/10.1016/j.saa.2011.02.042
28. M. Lucarini, P. Pedrielli, G.F. Pedulli, S. Cabiddu and C. Fattuoni, *J. Org. Chem.*, **61**, 9259 (1996); https://doi.org/10.1021/jo961039i
29. R.A. Jackson and K.M. Hosseini, *J. Chem. Soc. Chem. Commun.*, **13**, 967 (1992); https://doi.org/10.1039/C39920000967
30. D.D.M. Wayner, E. Lusztyk, K.U. Ingold and P. Mulder, *J. Org. Chem.*, **61**, 6430 (1996); https://doi.org/10.1021/jo952167u
31. E. Klein and V. Lukes, *J. Phys. Chem. A*, **110**, 12312 (2006); https://doi.org/10.1021/jp063468i
32. M. Nsangou, J.J. Fifen, Z. Dhaouadi and S. Lahmar, *J. Mol. Struct. THEOCHEM*, **862**, 53 (2008); https://doi.org/10.1016/j.theochem.2008.04.028
33. F. Martorana, M. Foti, A. Virtuoso, D. Gaglio, F. Aprea, T. Latronico, R. Rossano, P. Riccio, M. Papa, L. Alberghina and A.M. Colangelo, *Oxid. Med. Cell. Longev.*, **2019**, 1 (2019); https://doi.org/10.1155/2019/8056904
34. F.A.M. Silva, F. Borges, C. Guimaraes, J.L.F.C. Lima, C. Matos and S. Reis, *J. Agric. Food Chem.*, **48**, 2122 (2000); https://doi.org/10.1021/jf9913110
35. J.P. Tomasi and P.D. Truhlar, Chemical Application of Atomic and Molecular Electrostatic Potentials, Plenum: New York (1981).
36. M.N. Arshad, A.M. Asiri, K.A. Alamry, T. Mahmood, M.A. Gilani, K. Ayub and A.S. Birinji, *Spectrochim. Acta A Mol. Biomol. Spectrosc.*, **142**, 364 (2015); https://doi.org/10.1016/j.saa.2015.01.101
37. K. Fukui, T. Yonezawa and H. Shingu, *J. Chem. Phys.*, **20**, 722 (1952); https://doi.org/10.1063/1.1700523
38. K.O. Sulaiman and A.T. Onawole, *Comput. Theor. Chem.*, **1093**, 73 (2016); https://doi.org/10.1016/j.comptc.2016.08.014
39. C.J. Parkinson, P.M. Mayer and L. Radom, *J. Chem. Soc., Perkin Trans. 2*, **11**, 2305 (1999); https://doi.org/10.1039/a905476f
40. F. Weinhold and C.R. Landis, *Chem. Educ. Res. Pract.*, **2**, 91 (2001); https://doi.org/10.1039/B1RP90011K
41. M. Szafran, A. Komasa and E. Bartoszak-Adamska, *J. Mol. Struct. THEOCHEM*, **827**, 101 (2007); https://doi.org/10.1016/j.molstruc.2006.05.012
42. Y. Erdogdu, O. Unsalan, M. Amalanathan and I. Hubert Joe, *J. Mol. Struct.*, **980**, 24 (2010); https://doi.org/10.1016/j.molstruc.2010.06.032